Time-Dependent Response of the Large-Scale Solar Corona and Solar Wind*

Jon A. Linker, Roberto Lionello, Zoran Mikic, and Pete Riley

Science Applications International Corporation (SAIC)

San Diego, CA, USA

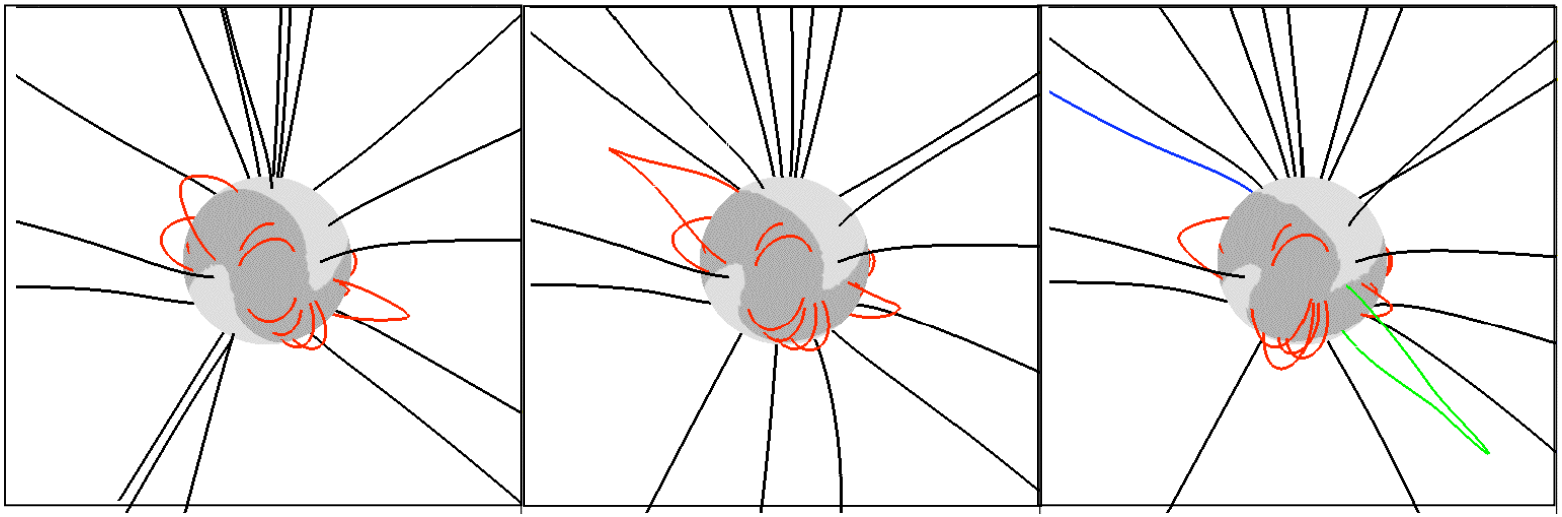

*Work supported by NASA and NSF

Introduction

- The solar magnetic field defines the structure of the solar corona and inner heliosphere
  - Heliospheric Current Sheet (HCS)
  - Fast and Slow Wind
- It is difficult to measure the coronal magnetic field
- Understanding coronal structure requires modeling $\Rightarrow$ use photospheric/chromospheric magnetic field as boundary conditions.
- Examples: Source-Surface (potential) model, MHD
- Despite their obvious limitations, steady-state models have been successful in describing many features of the corona and solar wind

Modeling the Corona and Solar Wind

- Steady-state models have had remarkable success in modeling different aspects of the corona and solar wind

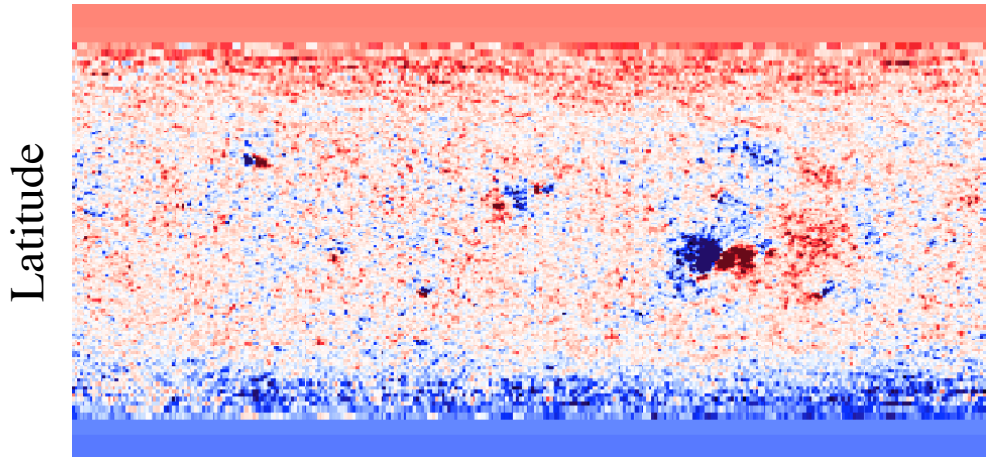

- The key input to these models is measurements of the line-of-sight photospheric magnetic field
- Examples: source-surface models, MHD models

MHD Equations

$$\nabla \times \mathbf{B} = \frac{4\pi}{c} \mathbf{J}$$

$$\nabla \times \mathbf{E} = -\frac{1}{c}\frac{\partial \mathbf{B}}{\partial t}$$

$$\mathbf{E} + \frac{1}{c} \mathbf{v} \times \mathbf{B} = \eta \mathbf{J}$$

$$\frac{\partial \rho}{\partial t} + \nabla \cdot (\rho \mathbf{v}) = 0$$

$$\rho \left(\frac{\partial \mathbf{v}}{\partial t} + \mathbf{v} \cdot \nabla \mathbf{v} \right) = \frac{1}{c} \mathbf{J} \times \mathbf{B} - \nabla p - \nabla p_w + \rho \mathbf{g} + \nabla \cdot (\nu \rho \nabla \mathbf{v})$$

$$\frac{\partial p}{\partial t} + \nabla \cdot (p \mathbf{v}) = (\gamma - 1)(-p \nabla \cdot \mathbf{v} + S)$$

The Polytropic Model

- Neglect thermal conduction, coronal heating, radiation loss, and Alfvén waves (set $p_w = 0$ and $S = 0$)
- Simulate these effects (crudely) by setting $\gamma = 1.05$ (Parker 1963)

Radial Velocity
Open and Closed Field Lines

Whole Sun Month

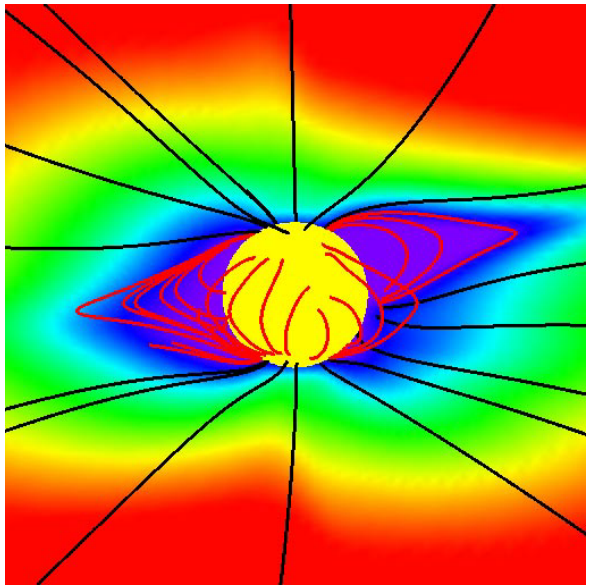

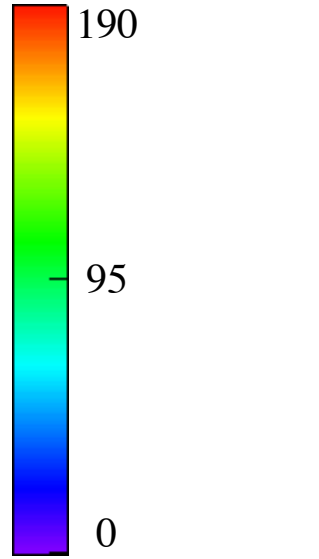

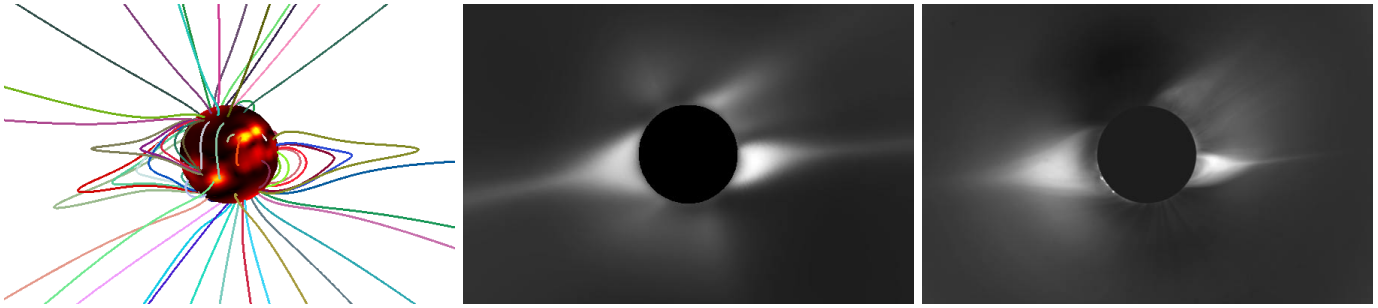

November 3, 1994 Solar Eclipse

Steady Solar Wind Models Can Describe Many Features of the Corona and Heliosphere

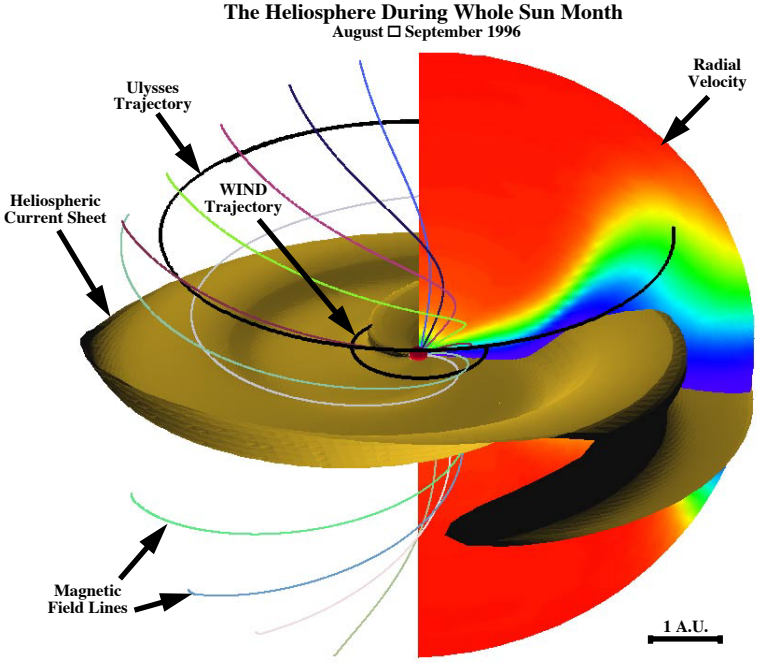

MHD Model of the Heliosphere during Whole Sun Month (empirical component)

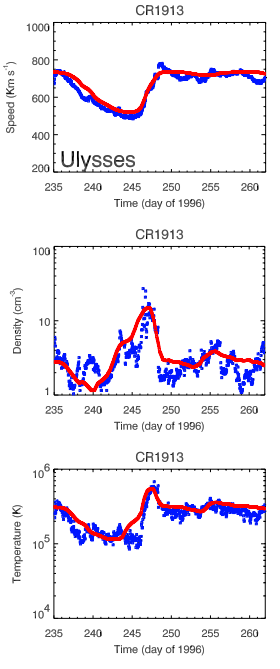

Comparison with Ulysses Observations

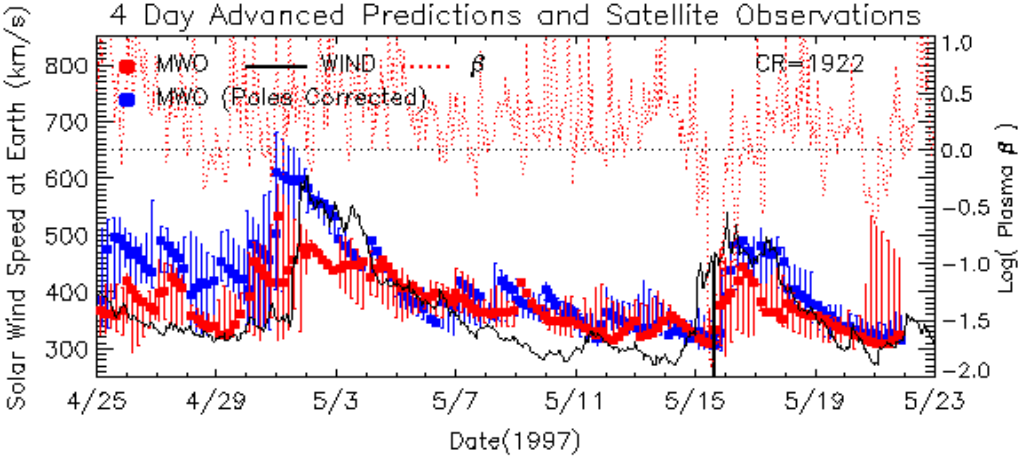

Arge-Wang-Sheeley Model

The Non-Steady Nature of the Ambient Corona and Solar Wind

- There are important features that cannot be understood from a steady-state approach
- Observations show that the closed field region cannot be static
- Examples:
  - Solar wind composition
  - Nearly rigid rotation of coronal holes

Solar Wind Composition contains important clues about dynamical processes in the Solar Corona

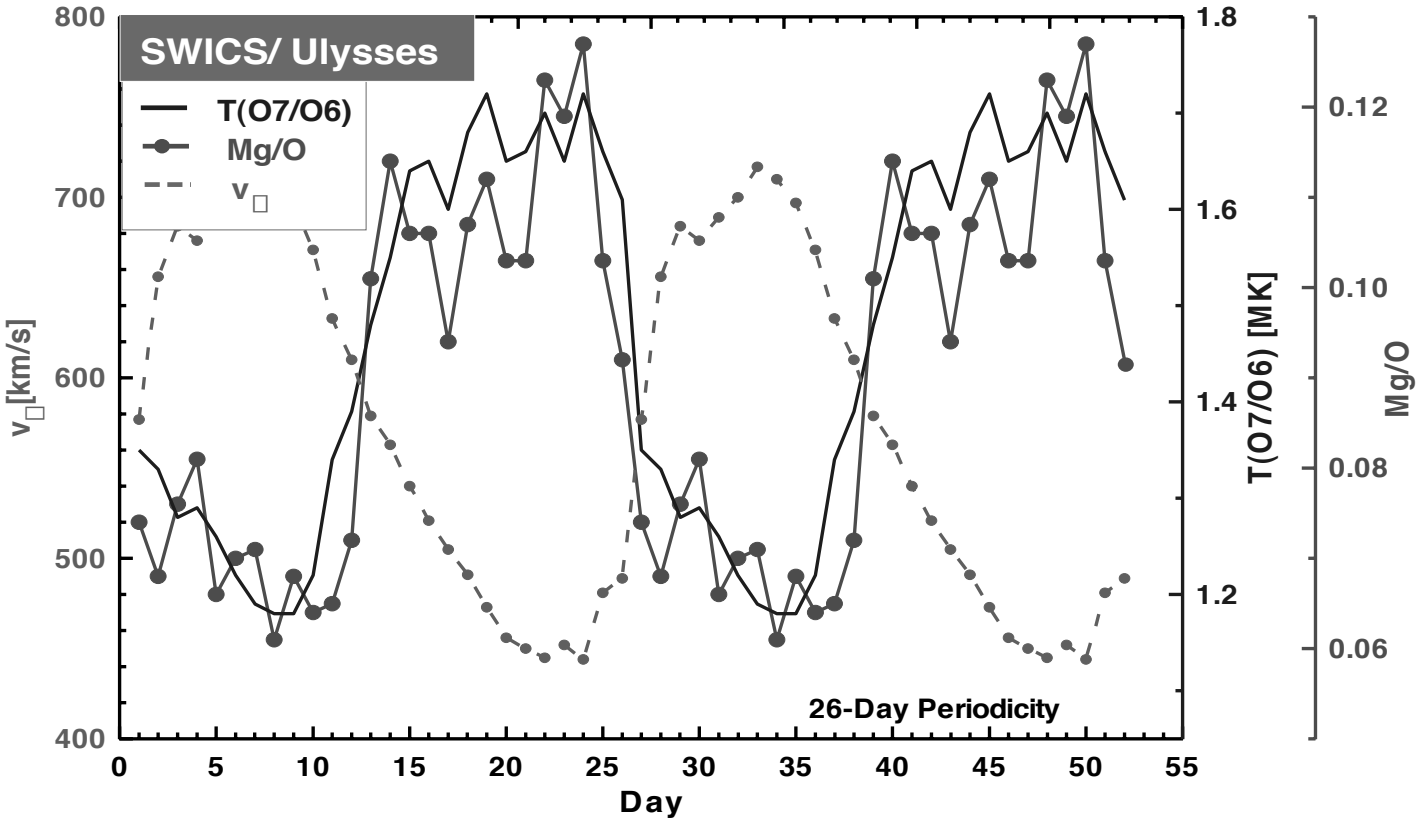

Superposed Epoch Analysis of Ulysses Data
Low-FIP, Plasma of Higher Temperature origin dominates in the Slow Solar Wind
(Geiss et al. 1995)

Implies that the plasmas making up the fast and slow wind have a different origin

Differential Rotation and Coronal Holes

- The sun rotates differentially (τ_{rot_eq} ~26 days, τ_{rot_pole} ~37 days)
- Differential rotation patterns clearly visible in B_{los} at photosphere
- Extended coronal holes often observed to rotate rigidly (first noticed in Skylab)
- Wang et al. (1996) provided explanation with simple model problem:
  - Bipolar active region embedded in a dipolar global field.
  - Sequences of source-surface (potential-field) models
  - Studied snapshots for 5 rotations
  - Implies continuous magnetic reconnection

Sequences of Potential Field Solutions

Snapshot from Schrijver &DeRosa sequence

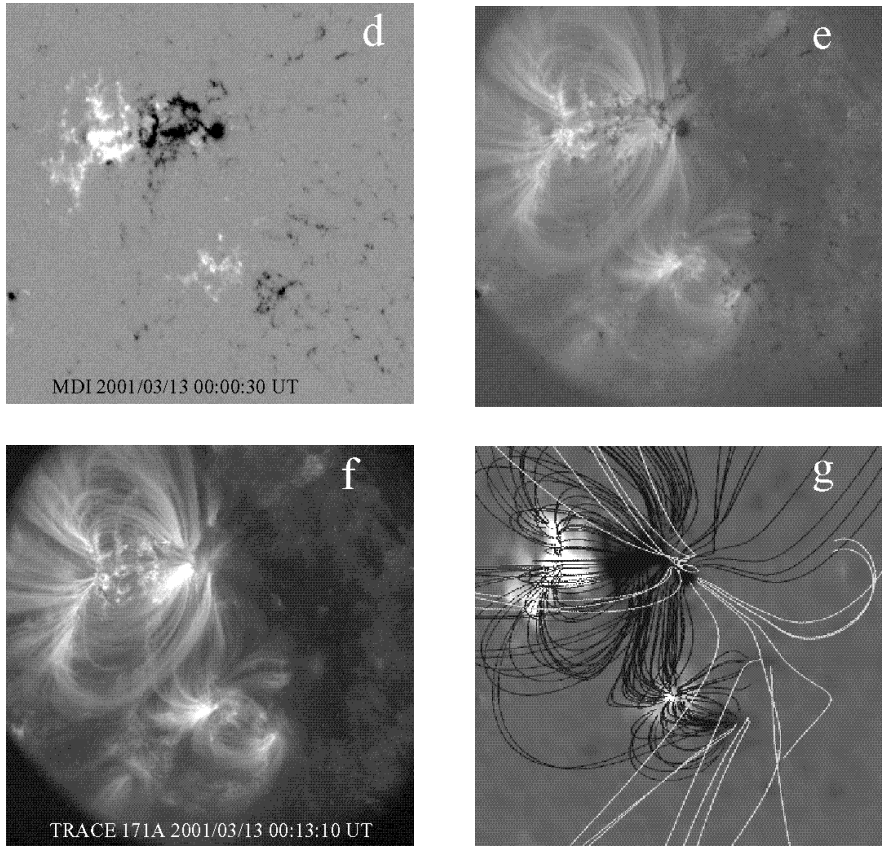

- Schrijver &DeRosa (2003):
  - Assimilated MDI magnetograms & photospheric flux evolution model
  - Source-surface model for each snapshot

Time-dependent Modeling

- Sequences of potential field models have been used to characterize the evolution of the coronal field.
- The sequences imply magnetic reconnection
- What is the nature of this reconnection?
- How do we reconcile apparently divergent pictures from coronal and heliospheric observations?

Reconnection of Coronal Magnetic Fields (Crooker et al. 2002)

a) Closed Loop Expands:
Bidirectional heat flux

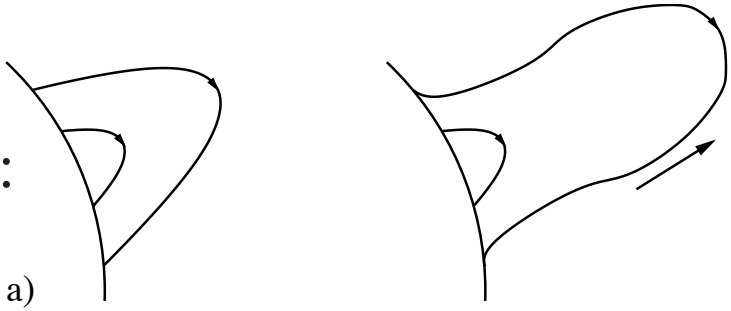

b) Two open field lines reconnect:
Heat flux dropouts (rare)

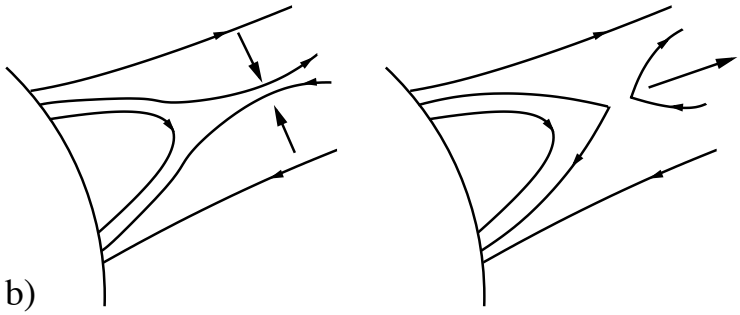

c) Interchange reconnection:
normal heat flux

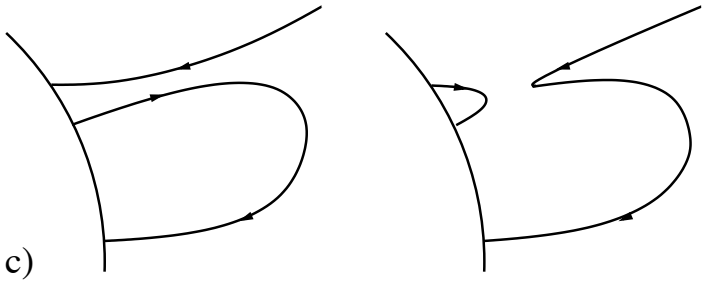

d) (Fisk et al:) Need to transport open flux during the course of the solar cycle;
can't create disconnected flux

Fisk et al. 1996
(CIR generated particles at high latitudes)

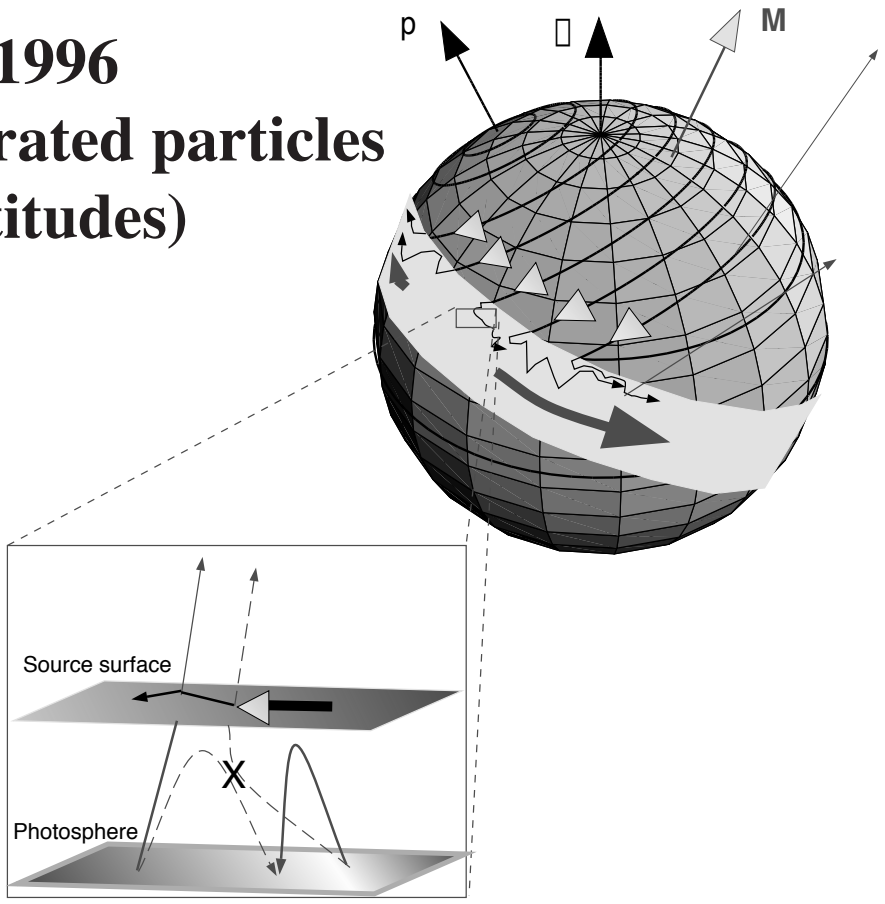

Fisk et al. key assumptions:
1) Field lines above Alfven point in magnetic pressure balance;
2) Coronal holes rotate rigidly;
3) Reconnection of field occurs below Alfven point.

Consequences:
1) Heliospheric field lines move in latitude;
2) Cannot create much disconnected flux, so *Reconnection must be between closed and open fields.*

Fisk Explanation of CIR Energetic Particles at High Latitude

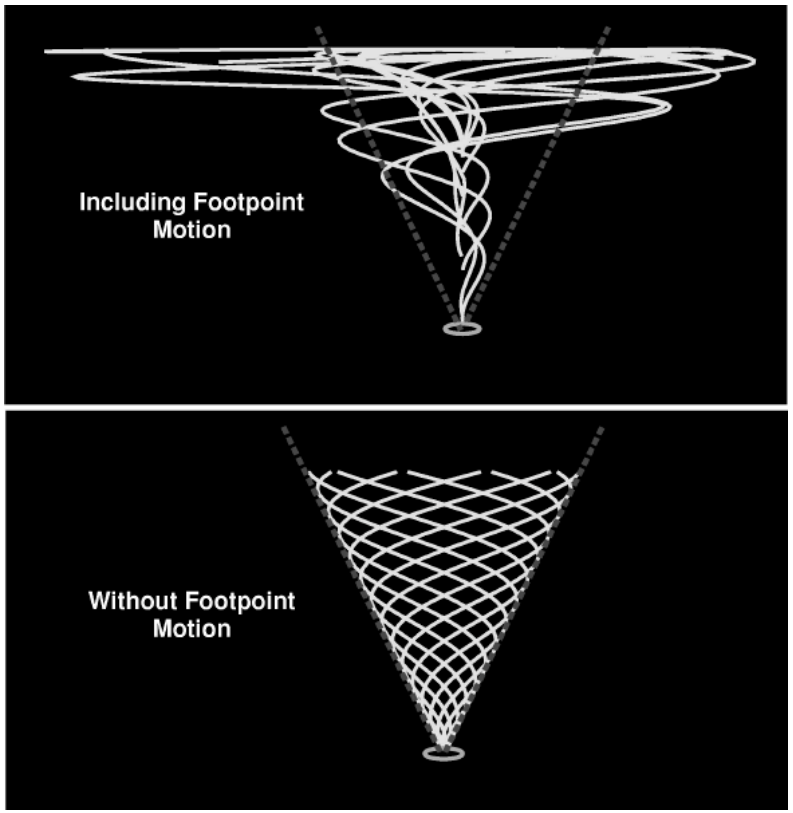

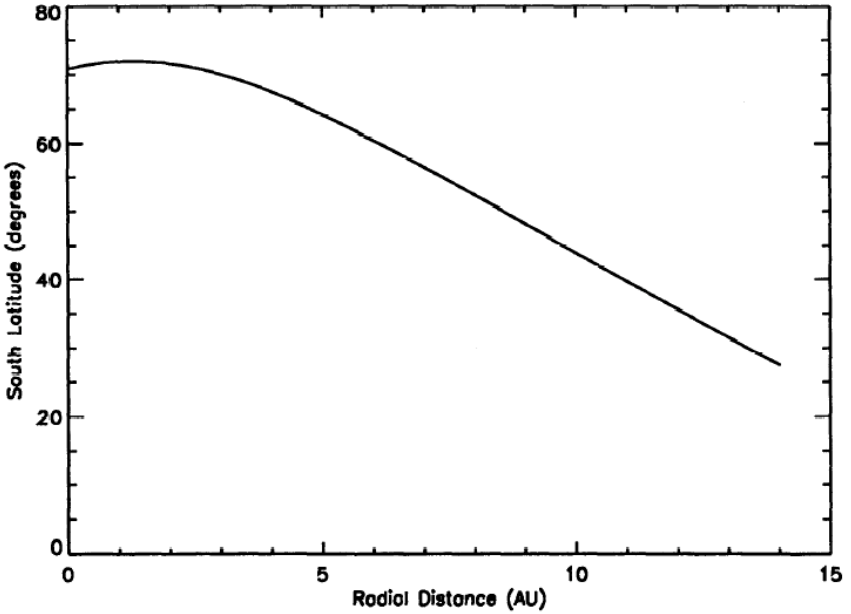

Figure 4. The heliographic latitude versus heliocentric distance of a field line which originates at 70° S latitude.

- Differential rotation allows field lines to move through region of rapid expansion
- Field lines at large distance sample a range of latitudes (outside the cone)

Time-Dependent Modeling of Coronal Field Evolution

- We (SAIC) are investigating time-dependent evolution
- Two model problems with differential rotation:
  - Axisymmetic dipole+bipolar active region (a la Wang)
  - Tilted dipole (Fisk)
- Time-dependent MHD
- Important caveat: $S_{simulation} << S_{corona}$
- Series of simulations for 5 solar rotations (~135 days):
  - Rotation rates from true to $10 \bullet \omega_{sun}$
  - Nonuniform meshes of 61×71×64 & 101×101×128
  - Performed in rotating frame of the Sun, but dropped coriolis terms
- Can we reconcile coronal and heliospheric points of view?

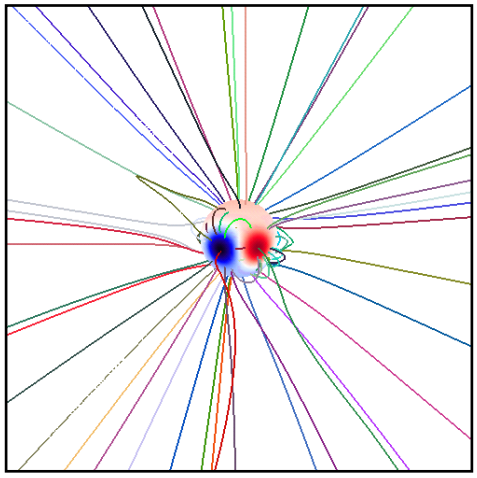

Streamer Configuration: Dipole plus a Large Active Region

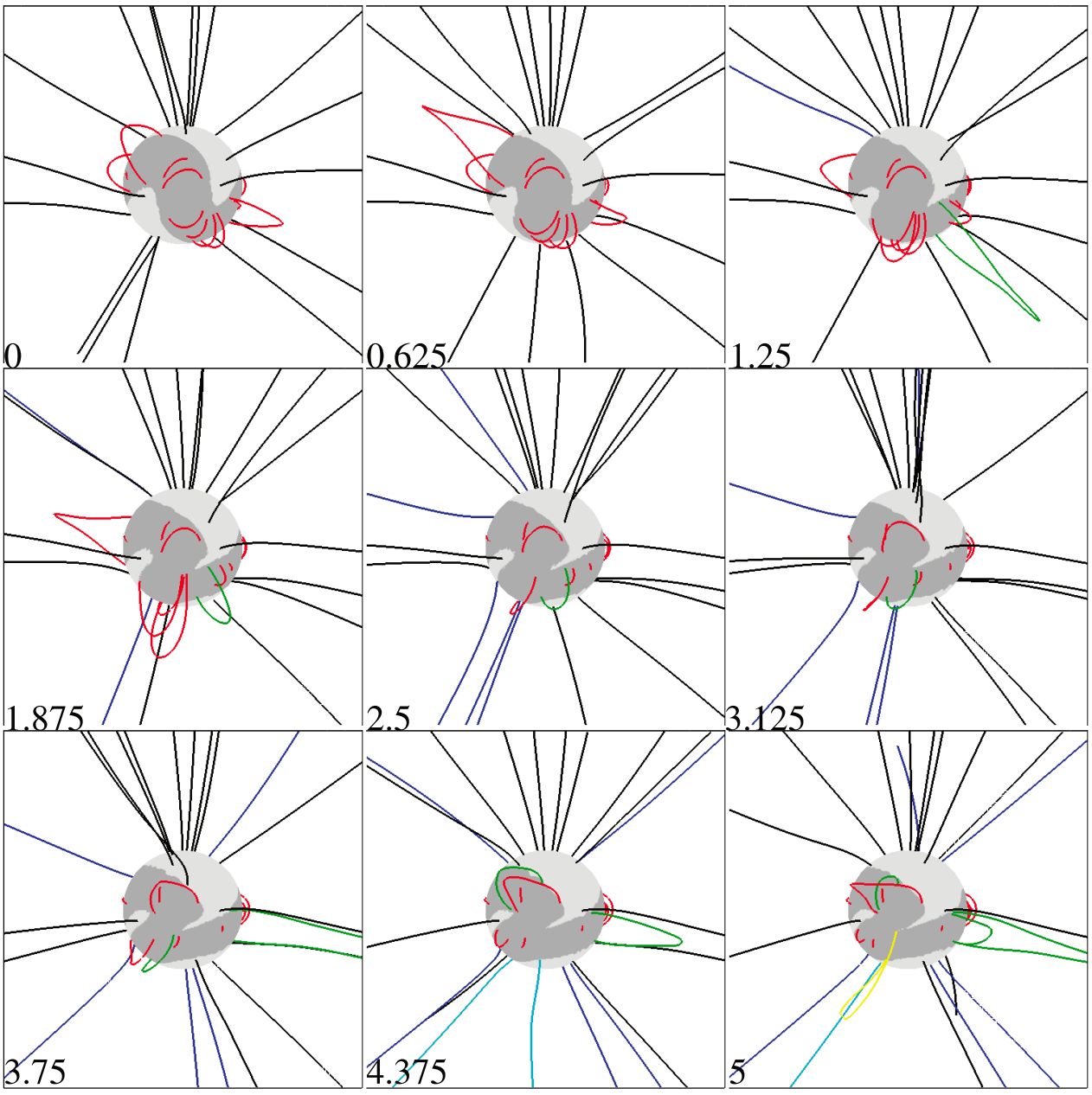

Coronal Hole Evolution Subject to Differential Rotation

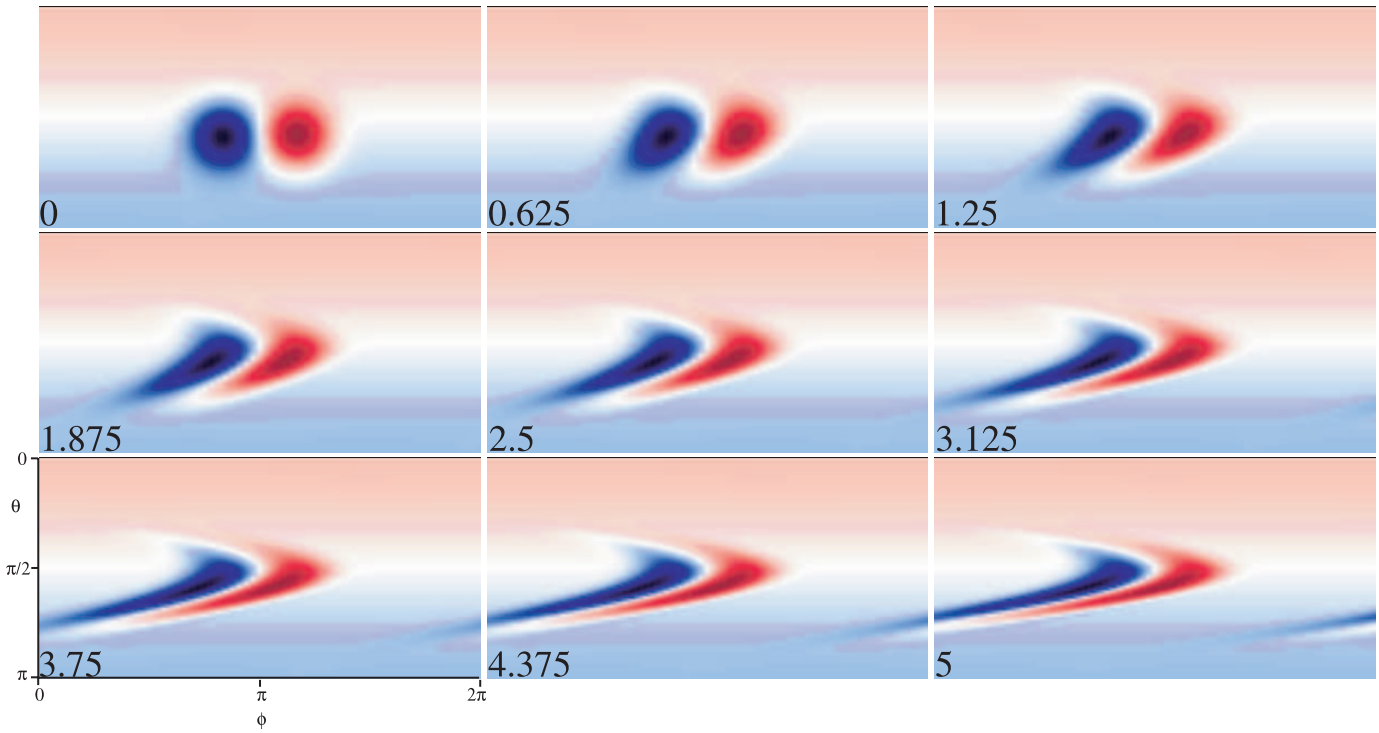

FIG. 1.—Sequence of projections showing the evolution of the radial component of the magnetic field during the simulation. The abscissae axis has the solar longitude, and the ordinates axis has the latitude. The time of each frame is measured in terms of fractional solar rotations.

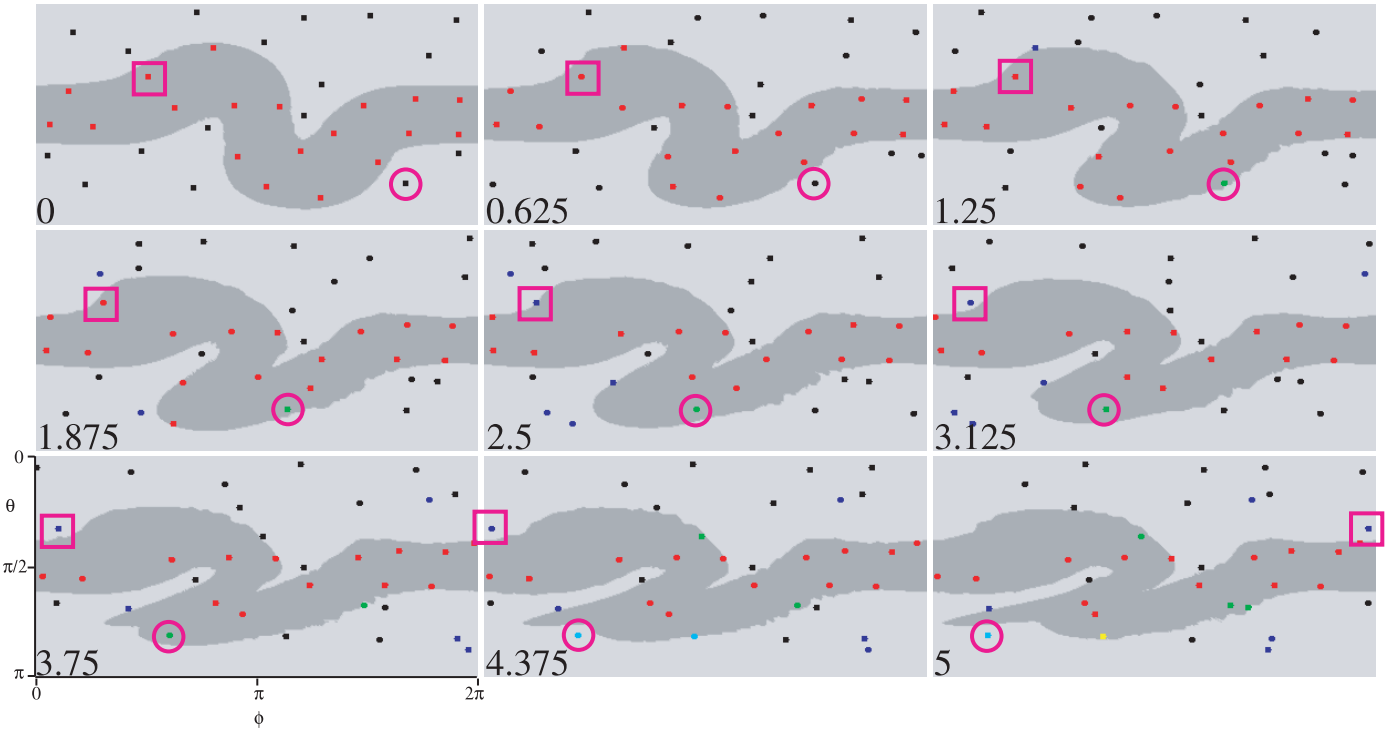

FIG. 2.—Sequence of projections showing the evolution of coronal holes boundaries during the simulation. The interval between the frames is the same as in Fig. 1. Dark gray areas are closed-field regions and those in light gray have open magnetic field. The dots represent field-line launch points that are advected by the shearing flow. Red launch points are associated with field lines that are initially closed; their color is changed to blue when the lines open up. Black launch points are associated with field lines that are initially open; their color is changed successively to green, cyan, and yellow as they close down, open up again, and close down for a second time, respectively. A black point has been enclosed by a circle to facilitate recognition as it moves into the closed-field region and then out of it, changing color after it crosses each boundary. Similarly, a red point, which moves out of the closed-field region into the northern coronal hole, has been enclosed in a box.

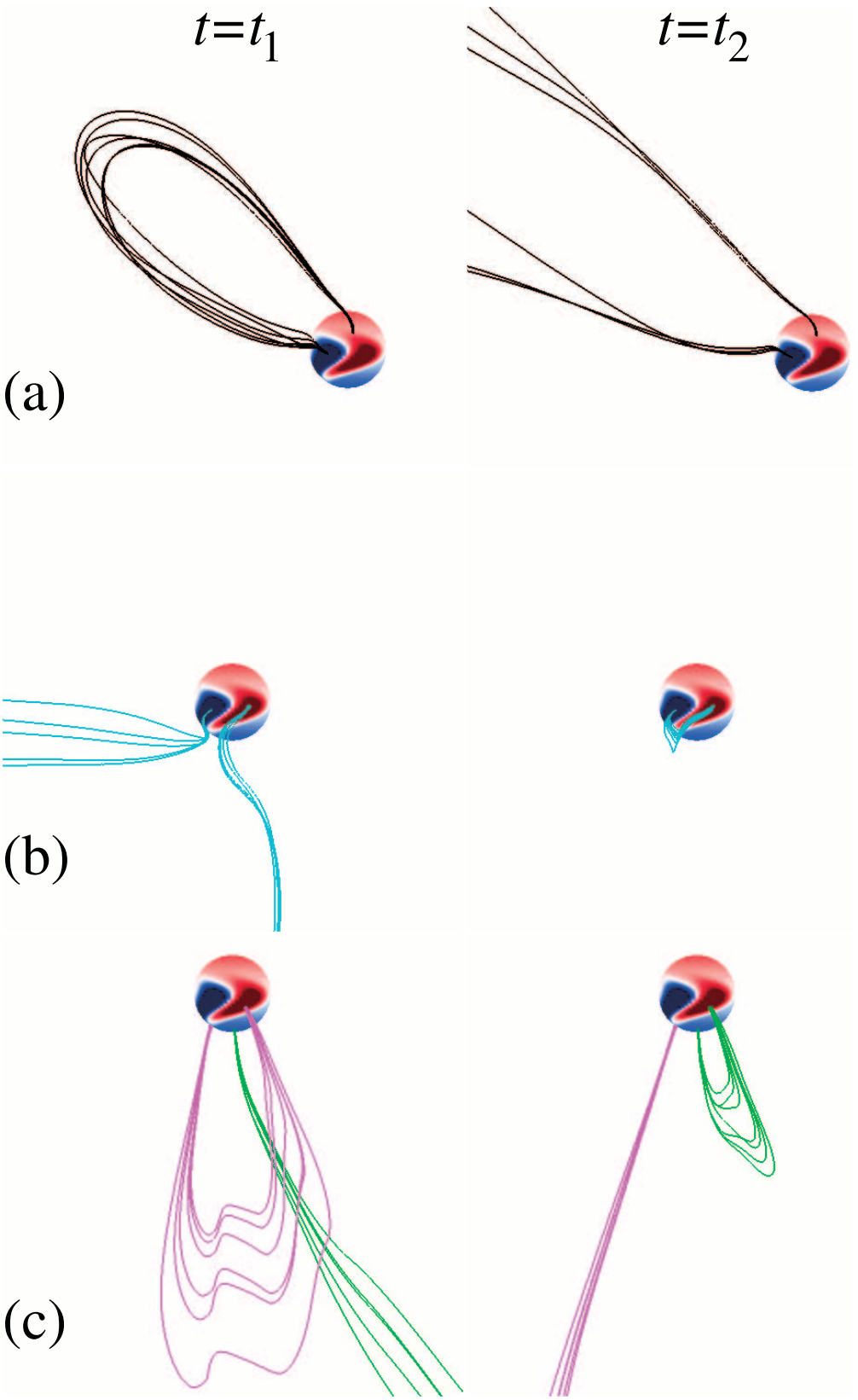

FIG. 5.—Reconnection events occurring during the simulation and serving as examples of the three types illustrated in Fig. 4. The time separation between frames is $t_2 - t_1 = 0.0625$ solar rotations. (*a*) Opening up of closed field lines; (*b*) reconnection of open field lines that form a loop; (*c*) interchange reconnection between closed and open field lines. The solar surface is color coded according to the magnetic flux (*red*: positive flux; *blue*: negative flux).

Field Line Connectivity vs. Time (snapshots every 0.6 rotations)

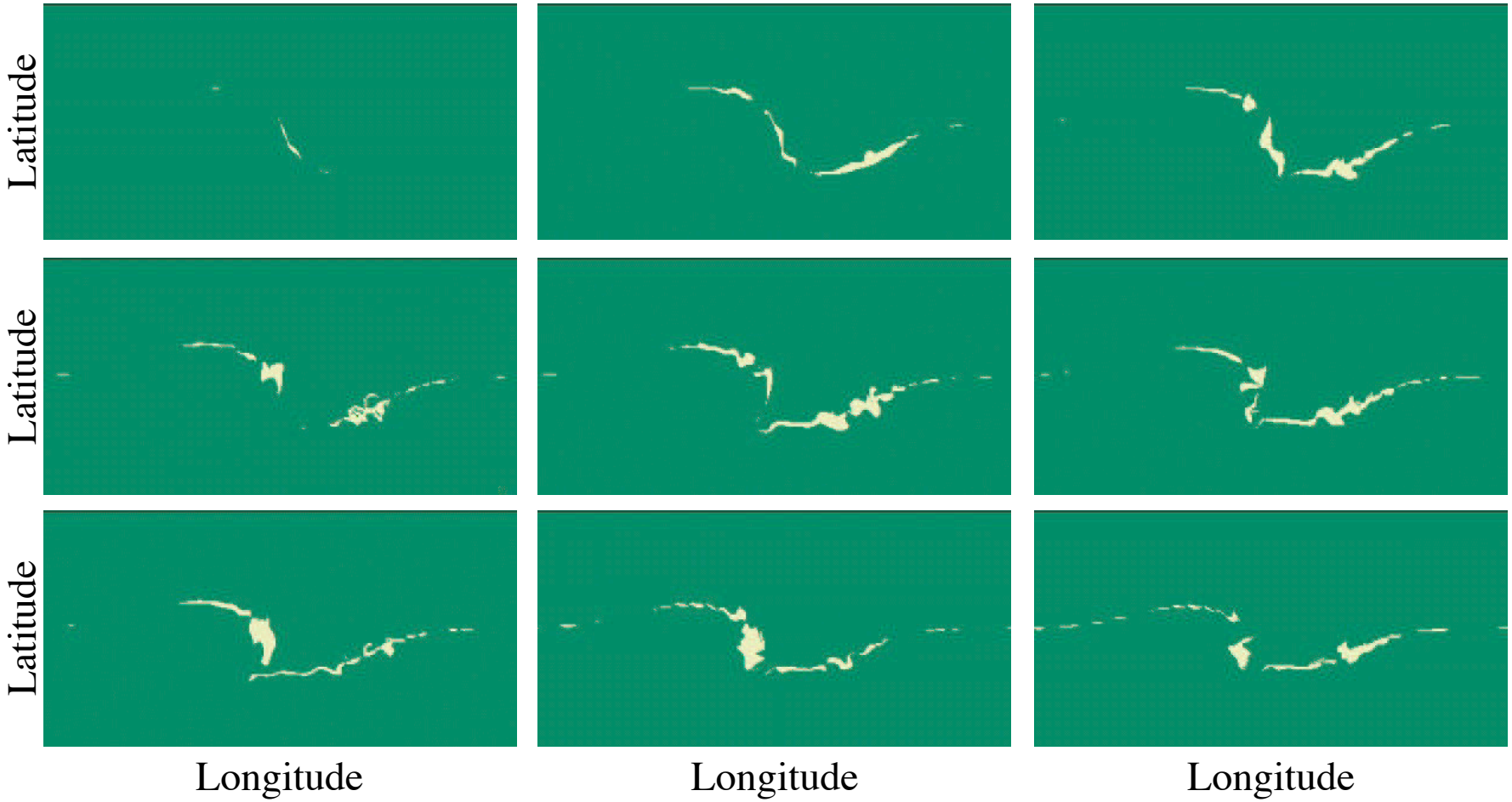

- Green regions: magnetic field connects back to the Sun from 30 R_s
- Yellow regions: Field is disconnected from the solar surface
- Disconnection region is entirely confined to heliospheric current sheet

Dipole+Bipolar AR Summary:

- MHD simulations of the differential rotation of a dipole+active region support many of the conclusions of Wang et al. (1996):
  - Northern polar coronal hole extension rotates more rigidly than southern
  - See Lionello et al. (2005) ApJ for details
- Interchange reconnection was identified in the simulation.
- Narrow disconnection events confined to HCS are also observed. Consistent with heliospheric data?

Differential Rotation of Tilted Dipole

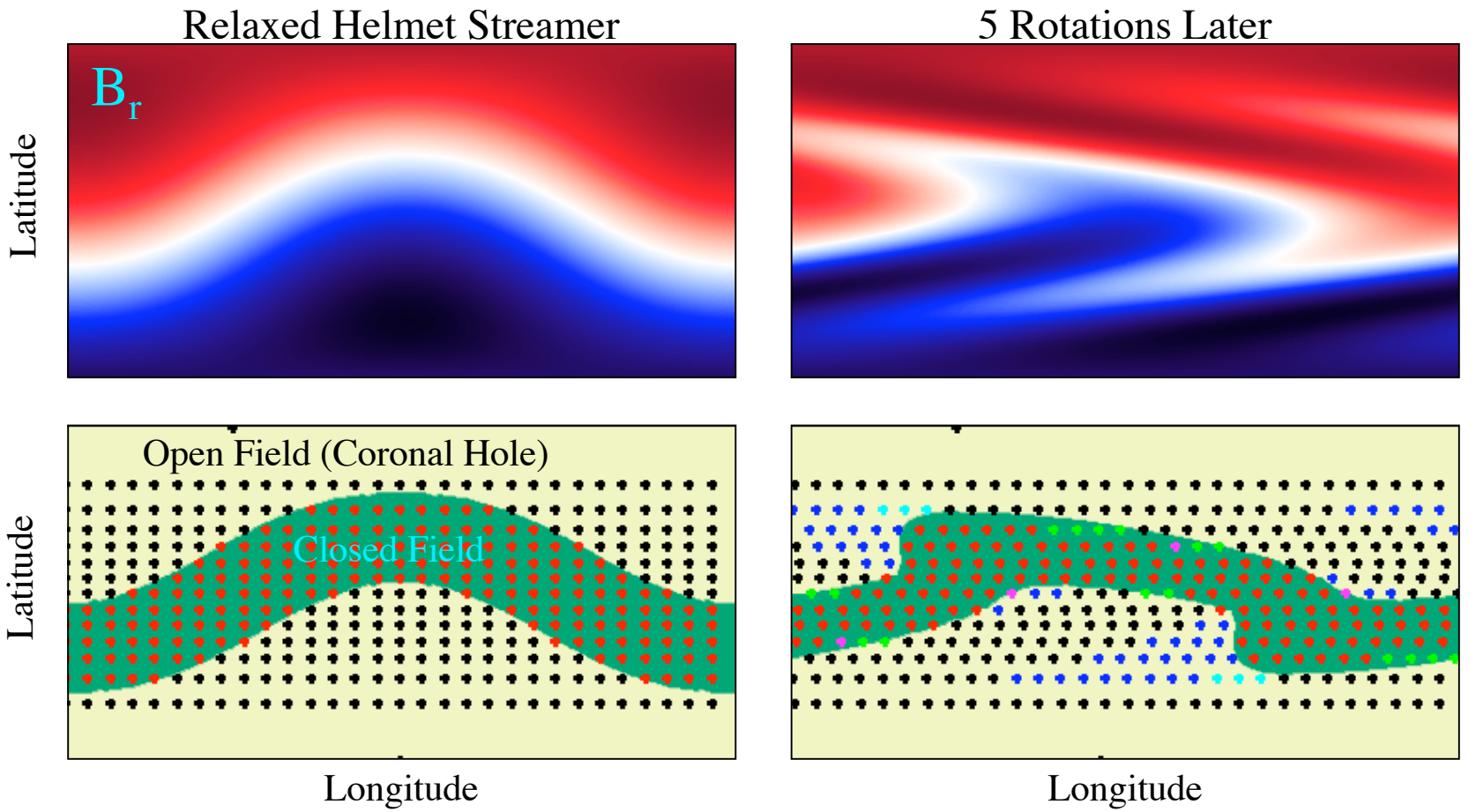

Topological Changes recorded at Magnetic Footpoints:

+ **Open** + **Closed** + **Closed⇒Open** + **Open ⇒ Closed**
+ **Open ⇒ Closed ⇒ Open** + **Closed ⇒ Open ⇒ Closed**

- Coronal hole pattern is far less distorted than $B_{r,}$, but not strictly rigid
- Reconnection of field lines occurs near the coronal hole boundaries.

Precession of Differential Rotating Field Lines

Relaxed Streamer

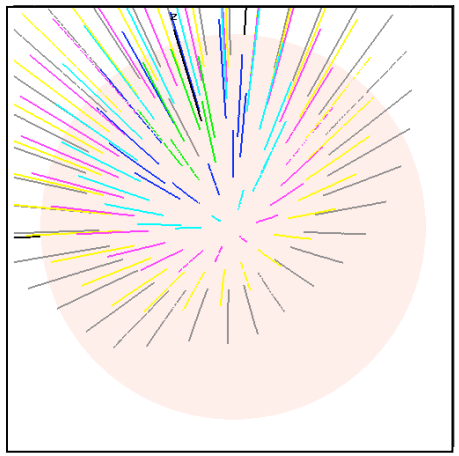

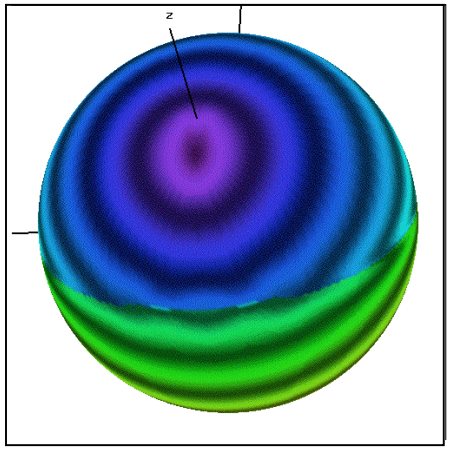

2.5 Rotations later

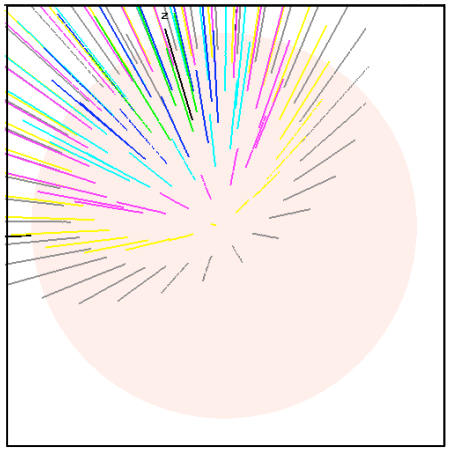

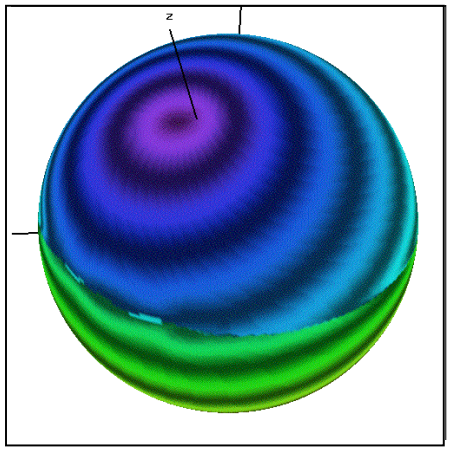

- Contrary to Fisk model, polar field line beyond Alfven point is not fixed
- Field lines precess rather than rotate about fixed polar field line
- Occurs because coronal hole boundary not strictly rigid
- Field lines beyond Alfven point do move in latitude

Latitude Sampling of Field Lines

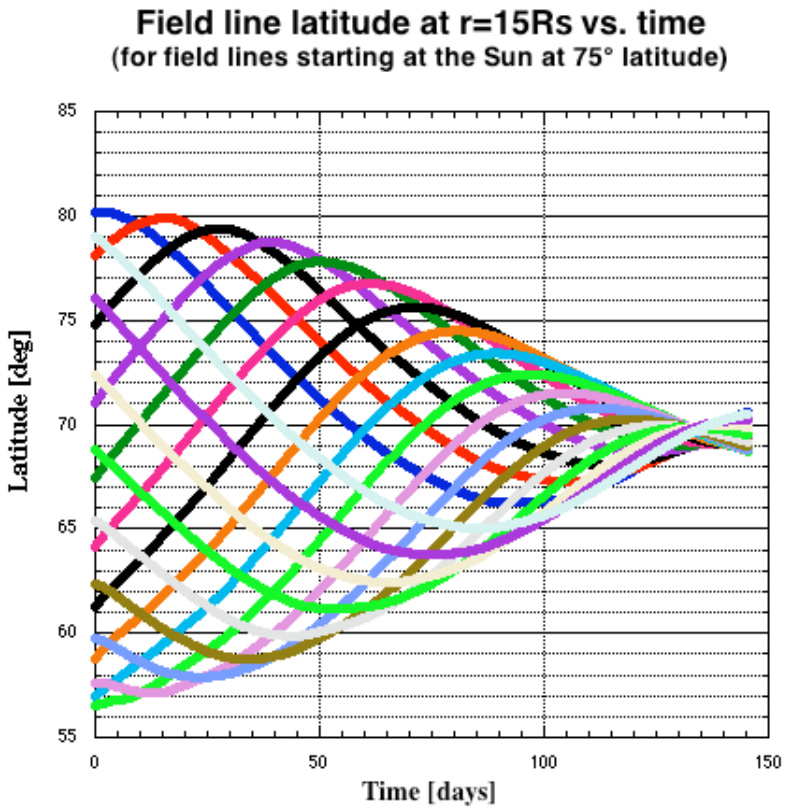

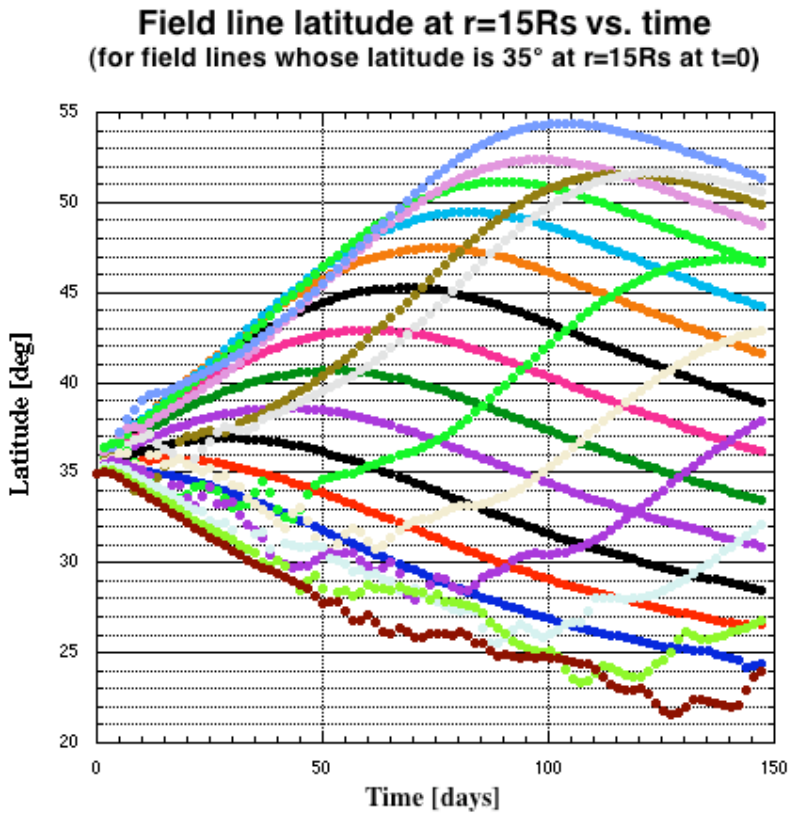

- Confirms basic idea of Fisk (1996)
- Maximum change in latitude ~25°
- Not enough to account for Ulysses observations

SUMMARY

- We have performed time-dependent MHD calculations of simple coronal configurations subject to differential rotation
- The calculations support Wang et al. (1996) explanation of the rigid rotation of some extended coronal holes
- The calculations support the basic idea of Fisk (1996) that open field lines move in heliographic latitude, however:
  - Assumption of strictly rigid rotation of coronal holes breaks down
  - Rotation is not fixed about an axis
  - Latitude traversal only ~25° (not enough to explain Ulysses data)
  - More realistic configuration could yield larger latitude variations
- Interchange reconnection occurs in simulations
- Disconnection also occurs ("not allowed in heliosphere")
  - Narrow, sporadic, and confined to HCS
  - Observable?

SUMMARY (continued)

- Time-dependent modeling of the ambient corona is still in an early stage
- It can help us obtain a deeper understanding of the connection between the Sun's magnetic field and the heliosphere
- We should attempt to model from actual magnetograms with a model of photospheric flux evolution

Extra Slides

What about Emerging Flux?

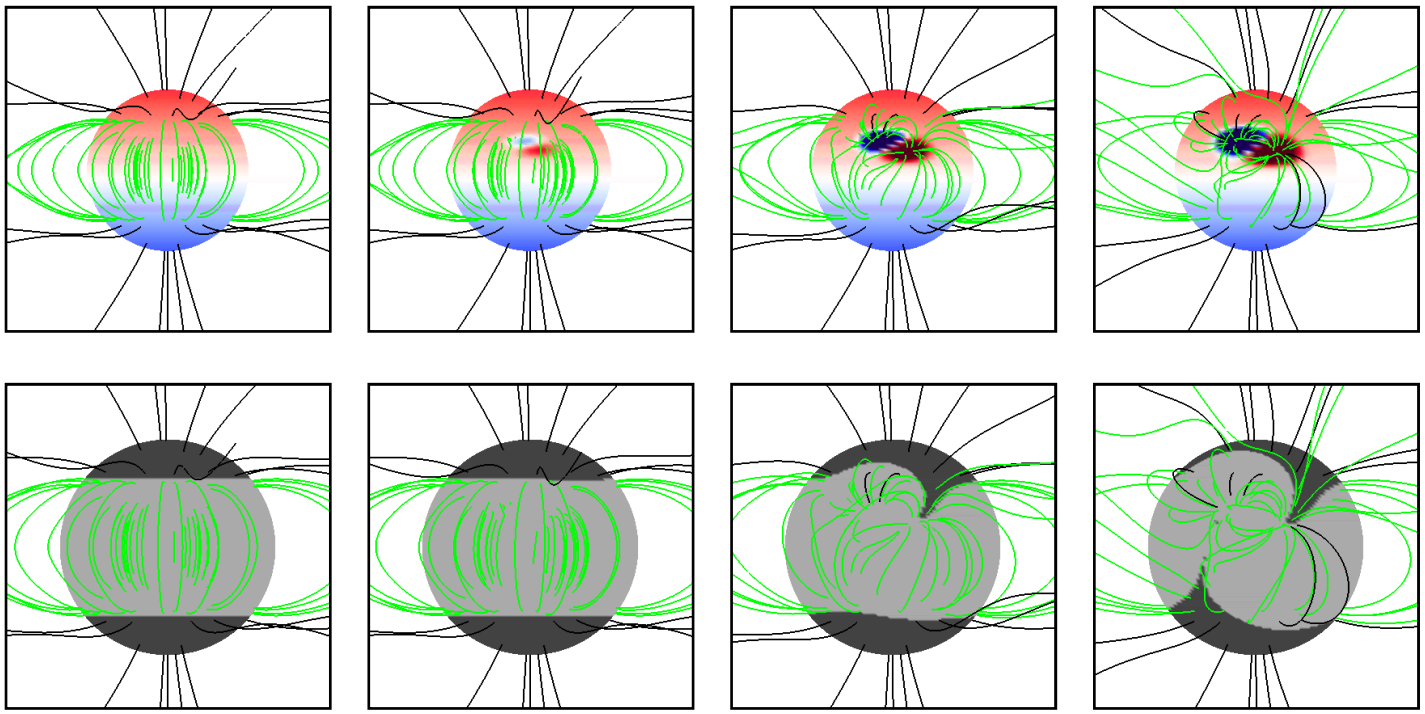

Emergence of a bipolar active region shows substantial changes in field connectivity: Needs to be studied in detail

Can be applied to real magnetograms.....

MHD EQUATIONS
(IMPROVED ENERGY EQUATION MODEL)

$$\nabla \times \mathbf{B} = \frac{4\pi}{c}\mathbf{J}$$

$$\nabla \times \mathbf{E} = -\frac{1}{c}\frac{\partial \mathbf{B}}{\partial t}$$

$$\mathbf{E} + \frac{1}{c}\mathbf{v} \times \mathbf{B} = \eta \mathbf{J}$$

$$\frac{\partial \rho}{\partial t} + \nabla \cdot (\rho \mathbf{v}) = 0$$

$$\rho\left(\frac{\partial \mathbf{v}}{\partial t} + \mathbf{v} \cdot \nabla \mathbf{v}\right) = \frac{1}{c}\mathbf{J} \times \mathbf{B} - \nabla p - \nabla p_w + \rho \mathbf{g} + \nabla \cdot (\nu \rho \nabla \mathbf{v})$$

$$\frac{\partial p}{\partial t} + \nabla \cdot (p\mathbf{v}) = (\gamma - 1)\left(-p\nabla \cdot \mathbf{v} - \nabla \cdot \mathbf{q} - n_e n_p Q(T) + H\right)$$

$$\gamma = 5/3$$

$$\mathbf{q} = -\kappa_{\parallel}\hat{\mathbf{b}}\hat{\mathbf{b}} \cdot \nabla T \qquad \text{(Close to the Sun, } r \lesssim 10R_S\text{)}$$

$$\mathbf{q} = 2\alpha n_e T\,\hat{\mathbf{b}}\hat{\mathbf{b}} \cdot \mathbf{v}/(\gamma - 1) \qquad \text{(Far from the Sun, } r \gtrsim 10R_S\text{)}$$

+ WKB equations for Alfvén wave pressure p_w evolution

Modeling the corona and solar wind: A more realistic energy equation

Log(Density)

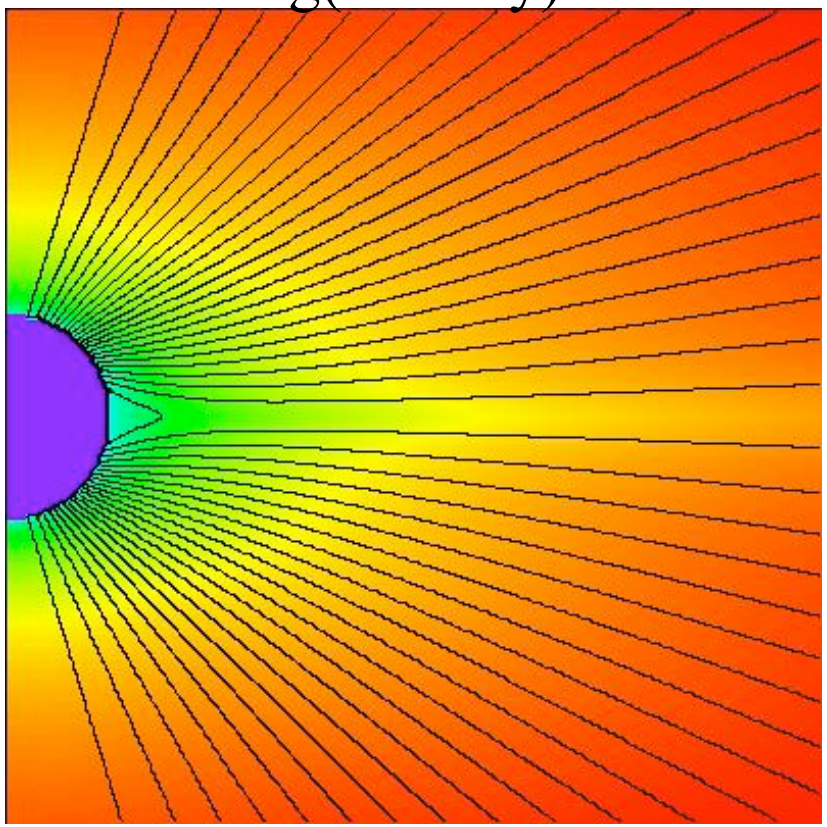

Range: 4 - 10

Temperature

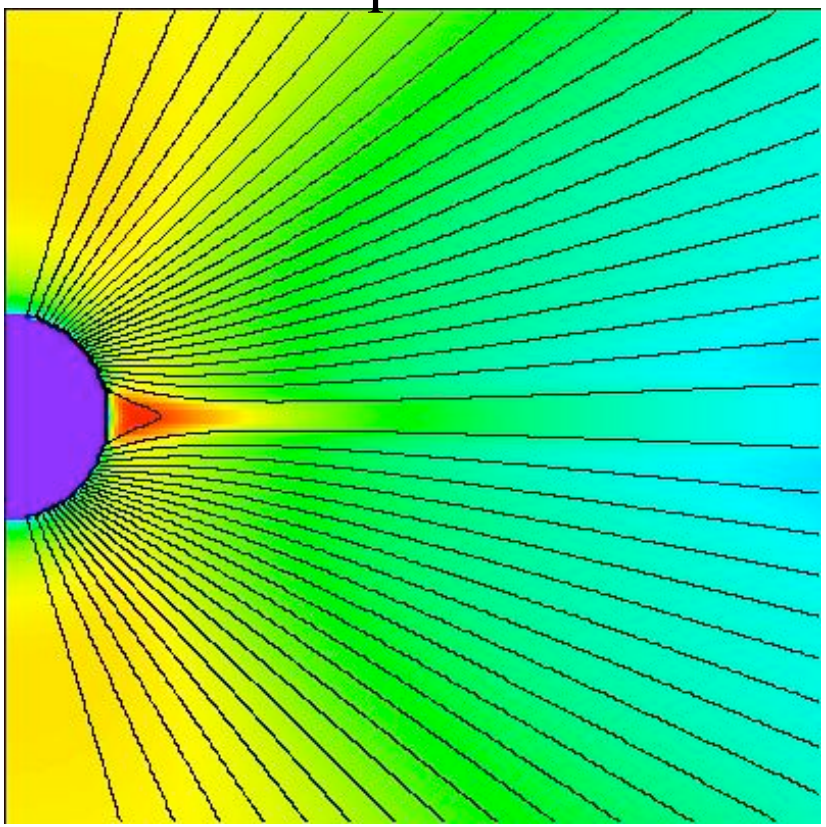

Range: 2E4 – 2E6 K

A more realistic energy equation (continued)

Radial Velocity
Range:
0 – 760 km/s

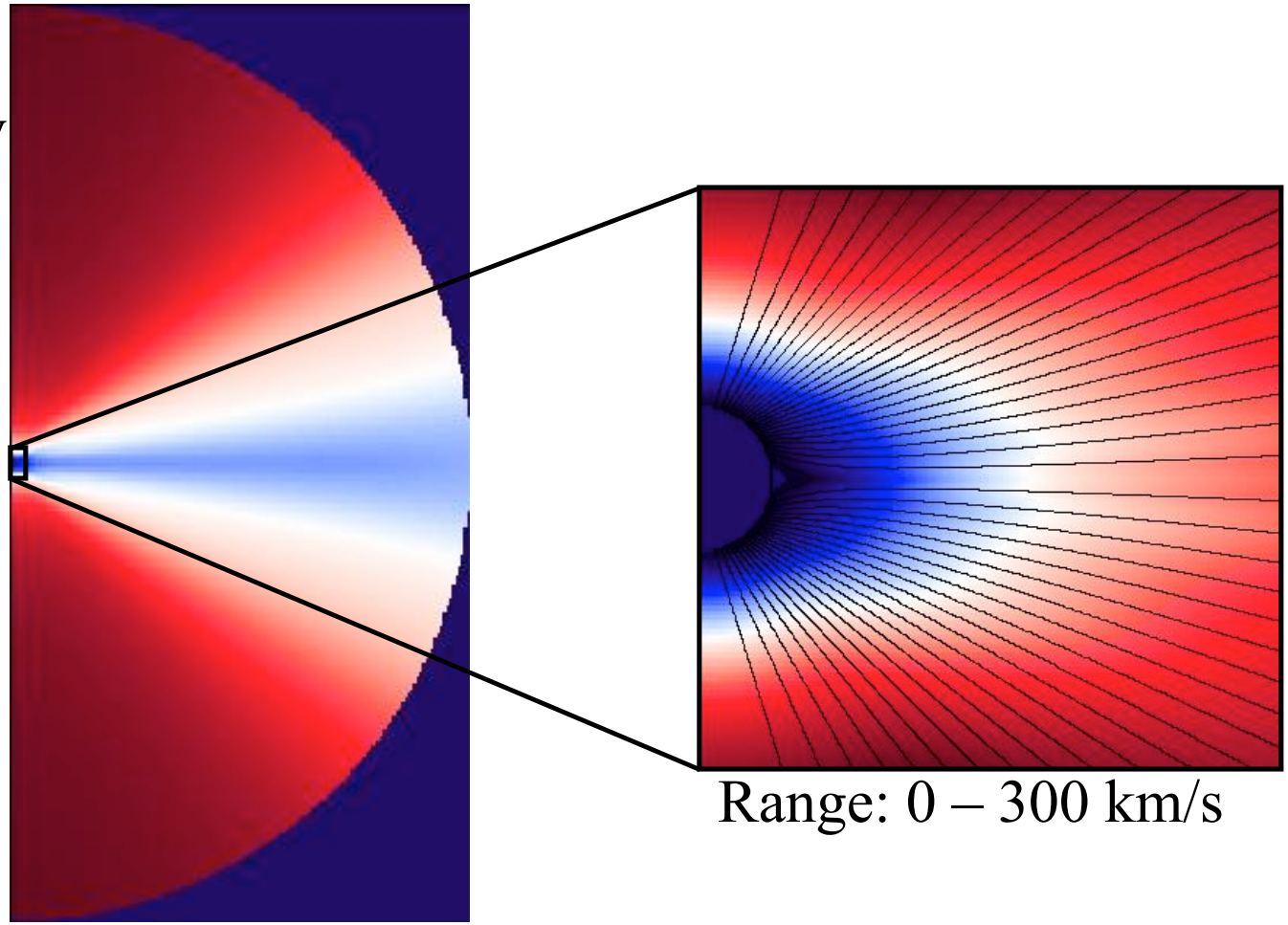

Range: 0 – 300 km/s